Determination of Propagation Constants and Wave Impedance of Non-Reciprocal Networks From Position-Insensitive Waveguide Measurements

Ugur C. Hasar, *Member, IEEE*, Yunus Kaya, Mucahit Izginli, Hamdullah Ozturk, Joaquim J. Barroso, *Member, IEEE*, Omar M. Ramahi, *Fellow, IEEE*, and Mehmet Ertugrul

***Abstract*— A microwave method is proposed to determine the forward and backward propagation constants (γ^+ and γ^-) and the wave impedance (z_w) of reciprocal and non-reciprocal microwave networks whose positions are not known within their measurement cells (position-insensitive). The proposed method relies purely on analytical expressions and can also evaluate the reference plane transformation distances. Scattering parameter measurements at the X-band (8.2–12.4 GHz) of a reciprocal network (a waveguide straight) and a non-reciprocal network (a microwave phase shifter) arbitrarily positioned into their measurement cells were conducted to retrieve γ^+, γ^-, and z_w for validation of our method and testing its position-insensitive property. The importance of the method becomes apparent when compared to conventional methods whose accuracy is based on precise determination of the reference planes.**

***Index Terms*— Non-reciprocal networks, position-insensitive, propagation constant, transmission and reflection methods, wave impedance.**

I. Introduction

ANALYSIS of electromagnetic properties of materials is an important research field through which physical, chemical, and mechanical properties of materials can be associated with their electromagnetic properties in various application areas such as agriculture [1], food engineering [2], and civil engineering [3]. In addition, information about electromagnetic properties of materials is also needed to customize their wave propagation characteristics (reflection, transmission, and refraction), such as electromagnetic cloaking [4] and superfocusing [5]. There are various methods available in the literature each with unique advantages to extract electromagnetic properties of materials. In selecting a suitable extraction methodology for a given application area, some criteria should first be specified such as accuracy, calibration requirement (calibration-dependent or calibration-free), suitability of the domain (time domain or frequency domain), type of testing (destructive versus nondestructive or invasive versus noninvasive), bandwidth (broadband or narrowband characterization), and accessibility (reflection-only or reflection–transmission measurements, or frequency shift or quality factor).

Among many microwave techniques (resonant and nonresonant) [6], our concern in this study is transmission–reflection nonresonant transmission-line or waveguide techniques [7]–[14]. Although these techniques are broadband, have a good accuracy, and require relatively less sample preparation (and labor), compared with resonant methods, they have three problems. The first problem is the numerical instability and/or increased measurement inaccuracy due to Fabry–Perot effect that may appear when the material behaves as a half-wave window (when the sample thickness L satisfies $L = n\lambda/2$ where λ is the wavelength inside the sample and n is an integer). This problem is significant in low-loss materials [10]. Iterative techniques [9], [15], noniterative technique [10], amplitude-only technique [13], and multiple-frequency approach [16] can be utilized to alleviate, if not totally eradicate, this problem. The second problem is the existence of nonunique solutions due to the branch index problem. The multiple-phase measurements [17], the group-delay technique [8], Kramers–Kronig relations [18], the phase-unwrapping technique [19], and the stepwise technique [20] can effectively be applied to evaluate the correct branch index or eliminate the branch index problem.

Besides, the third problem, which is our main interest in this study, of the transmission–reflection nonresonant methods is the need for transformation from the calibration-planes (the planes at which the measurement system is calibrated) to the measurement planes (the planes over which the sample's ends surfaces are located) for measurement configurations where the sample is small so that these planes do not overlap [9]. Such a transformation may degrade the

Manuscript received August 25, 2021; revised October 15, 2021; accepted October 23, 2021. Date of publication March 17, 2022; date of current version May 5, 2022. *(Corresponding author: Ugur C. Hasar.)*

Ugur C. Hasar and Hamdullah Ozturk are with the Department of Electrical and Electronics Engineering, Gaziantep University, 27310 Gaziantep, Turkey (e-mail: uchasar@gantep.edu.tr).

Yunus Kaya is with the Department of Electricity and Energy, Bayburt University, 69000 Bayburt, Turkey.

Mucahit Izginli is with the Department of Electrical and Electronics Engineering, Hasan Kalyoncu University, 27410 Gaziantep, Turkey.

Joaquim J. Barroso is with the Instituto Tecnológico de Aeronáutica, São José dos Campos 12228-900, Brazil.

Omar M. Ramahi is with the Department of Electrical and Computer Engineering, University of Waterloo, Waterloo, ON N2L 3G1, Canada.

Mehmet Ertugrul is with the Department of Electrical and Electronics Engineering, Ataturk University, 25240 Erzurum, Turkey, also with the Department of Electrical and Electronics Engineering, Universiti Putra Malaysia (UPM), Seri Kembangan, Selangor 43400, Malaysia, and also with the Faculty of Engineering, Kyrgyz-Turkish Manas University, Djal, Bishkek 720038, Kyrgyzstan.

Color versions of one or more figures in this article are available at https://doi.org/10.1109/TMTT.2022.3157718.

Digital Object Identifier 10.1109/TMTT.2022.3157718

performance of transmission–reflection methods, especially for high frequencies, if transformation factors (lengths L_{01} and L_{02} between calibration planes and the sample end surfaces) are not precisely known, which is generally the case when the sample is arbitrarily positioned in its measurement cell [21]. The recently proposed reference-plane-invariant or position-insensitive methods [21]–[35] can be used to remove the problems associated with such transformation. The methods [22]–[24], [34], [35] rely on amplitude-only information (reflection and/or transmission measurements) to extract relative complex permittivity ε_r of solid or liquid nondispersive or medium-level dispersive (low-loss to high-loss) materials. Although these methods require simple measurement instruments for recording amplitude information [no need to use complex scattering (S-) parameter measurements with an expensive vector network analyzer (VNA)], they are limited to dielectric samples only under the constraint that their frequency behavior (nondispersive or medium-level dispersive) must be known *a priori* if it follows a well-established frequency behavior such as the Debye and Lorentz models. To eliminate this constraint, complex S-parameter measurements can be applied [21], [25]–[33]. In [21] and [25]–[28], the electromagnetic properties (ε_r and the relative complex permeability μ_r) of solid or liquid dielectrics or magnetic samples were extracted without resorting to the determination of the reference plane transformation factors. The method in [32] was based on training of the measurement system via artificial neural networks, whereas the method in [33], which uses phasor matching algorithm, first determines the distances between the calibration and reference planes and then evaluates ε_r and μ_r of the dielectric/magnetic materials. In the case that reflection measurements can introduce errors into the ε_r and μ_r measurements of low-loss dielectric/magnetic materials, the method in [31] was proposed to mitigate the Fabry–Perot effects using position-invariant transmission and short-circuited reflection measurements. Furthermore, the methods in [21]–[28] and [31]–[35] can suffer from imperfect calibration standard used in the calibration process of the measurement setup. To reduce the effect of such calibration standard errors on ε_r and μ_r of solid samples, the methods in [29] and [30] can be conveniently employed. However, all the aforementioned reference-plane-invariant or position-insensitive methods require that the sample should be reciprocal and thus are not feasible for extraction of electromagnetic properties of non-reciprocal materials that find applications in microwave phase shifters [36] and chiral (meta)materials [37]. Our recent studies, which are used to characterize electromagnetic properties, propagation constant, and/or impedance of non-reciprocal samples, assume that the non-reciprocal sample fully fills the whole measurement cell [38]–[40]. In other words, these methods [37]–[40] require the information about reference planes for smaller samples within measurement cell and thus are position-dependent techniques.

In this study, we propose a position-insensitive transmission–reflection extraction method for obtaining forward and backward propagation constants and wave impedance of reciprocal and non-reciprocal samples. The organization of the remainder of this article is as follows. First, a theoretical background is given in Section II. In Section III, our method for extraction of propagation constants and wave impedance of a non-reciprocal network without resorting to reference plane transformation distances (position-insensitive property) is presented. In this section, expressions to determine these distances are also included to show the effectiveness of our formalism. In Section IV, measurement results of two different types of experiments are presented to validate the proposed method (using measurements of a reciprocal waveguide section) and to compare its accuracy with another method (using measurements of a non-reciprocal waveguide phase shifter), which requires *a priori* knowledge of reference plane transformation distances. In Section V, uncertainty analysis is applied to evaluate the performance of the proposed method and suggestions are made to enhance accuracy. Finally, all main findings are summarized in Section VI.

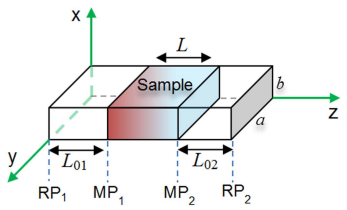

Fig. 1. Non-reciprocal sample with length L arbitrarily positioned at measurement planes MP_1 and MP_2 into the measurement cell calibrated to the reference (calibration) planes RP_1 and RP_2.

II. Theoretical Background

Fig. 1 shows a schematic view of a non-reciprocal sample with length L arbitrarily positioned (L_{01} and L_{02} are not known *a priori*) into a waveguide measurement cell with length $L_g = L_{01}+L+L_{02}$. It is assumed that the measurement cell is calibrated up to the reference planes RP_1 and RP_2 and that the sample is reflection-symmetric (having the same physical structure seen on both sides, such as the homogeneous chiral slab [37]) and fully fills the entire cross section ($-a/2 < x < a/2$ and $-b/2 < y < b/2$) of the waveguide cell operated at its dominant mode (TE_{10}). We consider the time dependence in the form of $\exp(+j\omega t)$ in the theoretical analysis.

The wave-cascading matrices (WCMs) of the measurement cell without the sample and with the sample can be, respectively, written as [29] and [30]

$$M_{\text{air}} = \frac{1}{S_{21}^{\text{air}}}\begin{bmatrix} \left(S_{21}^{\text{air}}S_{12}^{\text{air}} - S_{11}^{\text{air}}S_{22}^{\text{air}}\right) & S_{11}^{\text{air}} \\ -S_{22}^{\text{air}} & 1 \end{bmatrix} \tag{1}$$

$$M_{\text{cell}} = \frac{1}{S_{21}^{\text{cell}}}\begin{bmatrix} \left(S_{21}^{\text{cell}}S_{12}^{\text{cell}} - S_{11}^{\text{cell}}S_{22}^{\text{cell}}\right) & S_{11}^{\text{cell}} \\ -S_{22}^{\text{cell}} & 1 \end{bmatrix} \tag{2}$$

where S_{kl}^{air} and S_{kl}^{cell} (k and l: 1 and 2) are the S-parameters of the empty cell and the cell with sample, respectively.

The WCMs of the air- and sample-filled regions in Fig. 1 can be written as [39], [40]

$$T_{01(2)} = \frac{1}{\alpha_{01(2)}}\begin{bmatrix} \alpha_{01(2)}^2 & 0 \\ 0 & 1 \end{bmatrix}, \quad T_0 = \frac{1}{\alpha_0}\begin{bmatrix} \alpha_0^2 & 0 \\ 0 & 1 \end{bmatrix} \tag{3}$$

$$T_S = \frac{1}{T^+\left(1-\Gamma^2\right)}\begin{bmatrix} T^+T^- - \Gamma^2 & \Gamma\left(1-T^+T^-\right) \\ -\Gamma\left(1-T^+T^-\right) & 1-\Gamma^2T^+T^- \end{bmatrix} \tag{4}$$

$$\alpha_{01(2)} = e^{-jk_0\sqrt{1-(f_c/f)^2}L_{01(2)}}, \quad T^+ = e^{-\gamma^+ L} \tag{5}$$

$$\alpha_0 = e^{-jk_0\sqrt{1-(f_c/f)^2}L}, \quad T^- = e^{-\gamma^- L} \tag{6}$$

$$\Gamma = (z_w - 1)/(z_w + 1) \tag{7}$$

where T_{01} (α_{01}), T_{02} (α_{02}), and T_0 (α_0) are the WCMs (propagation factors) of the air-filled regions with lengths L_{01}, L_{02}, and L, respectively; T_S is the WCM of the sample-filled region with length L; T^+ and T^- are the propagation factors of the sample in the forward ($+z$) and backward ($-z$) directions; γ^+ and γ^- are the propagation constants in the forward ($+z$) and backward ($-z$) directions; Γ is the reflection coefficient at the air-sample interface; z_w is the normalized wave impedance of the non-reciprocal sample; $k_0 = \omega/c$ is the free-space wavenumber; $\omega = 2\pi f$ is the angular frequency; f is the linear frequency; and c is the velocity of light in air. Our goal is to extract T^+, T^-, and Γ (then γ^+, γ^-, and z_w) of the non-reciprocal sample without knowing L_{01} and L_{02}.

III. Proposed Method

Using WCMs in (1)–(4), it is possible to write

$$M_{\text{cell}}M_{\text{air}}^{-1} = T_{01}T_S T_0^{-1}T_{01}^{-1} = \begin{bmatrix} m_{11} & m_{12} \\ m_{21} & m_{22} \end{bmatrix} \tag{8}$$

$$M_{\text{cell}}^{-1}M_{\text{air}} = T_{02}^{-1}T_S^{-1}T_0 T_{02} = \begin{bmatrix} u_{11} & u_{12} \\ u_{21} & u_{22} \end{bmatrix} \tag{9}$$

where m_{kl} and u_{kl} are the entries (known from measurements) of the matrices $M_{\text{cell}}M_{\text{air}}^{-1}$ and $M_{\text{cell}}^{-1}M_{\text{air}}$, respectively.

A. Determination of Propagation Factors T^+ and T^- and Reflection Coefficient Γ

Using (8) and (9), it is possible to obtain

$$\frac{1}{\alpha_0 T^+\left(1-\Gamma^2\right)}\begin{bmatrix} T^+T^- - \Gamma^2 & \alpha_0^2\Gamma(1-T^+T^-) \\ -\Gamma(1-T^+T^-) & \alpha_0^2\left(1-\Gamma^2 T^+T^-\right) \end{bmatrix} = \frac{1}{\alpha_{01}^2}\begin{bmatrix} \alpha_{01}^2 m_{11} & m_{12} \\ \alpha_{01}^4 m_{21} & \alpha_{01}^2 m_{22} \end{bmatrix} \tag{10}$$

$$\frac{1}{\alpha_0 T^-\left(1-\Gamma^2\right)}\begin{bmatrix} T^+T^- - \Gamma^2 & \alpha_0^2\Gamma(1-T^+T^-) \\ -\Gamma(1-T^+T^-) & \alpha_0^2\left(1-\Gamma^2 T^+T^-\right) \end{bmatrix} = \frac{1}{\alpha_{02}^2}\begin{bmatrix} \alpha_{02}^2 u_{11} & \alpha_{02}^4 u_{12} \\ u_{21} & \alpha_{02}^2 u_{22} \end{bmatrix}. \tag{11}$$

From (10) to (11), it is possible to determine

$$\frac{\Gamma^2\left(1-T^+T^-\right)^2}{T^+T^-\left(1-\Gamma^2\right)^2} = \alpha_0^2\alpha_{01}^2\alpha_{02}^2 m_{21}u_{12} = A \tag{12}$$

$$\frac{\left(1-\Gamma^2 T^+T^-\right)^2}{T^+T^-\left(1-\Gamma^2\right)^2} = \frac{1}{\alpha_0^2}m_{22}u_{11} = C. \tag{13}$$

It is seen from (12) to (13) that A and C terms are known quantities, provided that the sample length L is known [33]. It is noted that when the sample is reciprocal ($T^+ = T^- = T$), the left-hand side of the expression of A in (12) is identical to that in (12) of the study [21] (for this reason, we used the same quantity) because $m_{21} = -S_{22}/(S_{21}\alpha_{01}^2\alpha_0)$ and $u_{12} = -S_{11}/(S_{21}\alpha_{02}^2\alpha_0)$, which are derived from (8) to (9). On the other hand, for a reciprocal sample, the left-hand side of the expression for C is different from that in (13) of the same study (different quantities).

Γ^2 can be evaluated from (13) as

$$\Gamma^2 = \frac{1-\sqrt{CT^+T^-}}{T^+T^- - \sqrt{CT^+T^-}}. \tag{14}$$

Substituting Γ^2 in (14) into (12), we have

$$T^+T^- + 2\xi_1\sqrt{T^+T^-} + 1 = 0, \tag{15}$$

$$\sqrt{T^+T^-} = -\xi_1 \mp \sqrt{\xi_1^2 - 1}, \quad \xi_1 = \frac{A-C-1}{2\sqrt{C}}. \tag{16}$$

The correct sign for $\sqrt{T^+T^-}$ in (16) can be evaluated by applying the passivity principle, that is, $|\sqrt{T^+T^-}| \leq 1$, where $|\star|$ denotes the magnitude of "$\star$." Next, T^+T^- term is computed by squaring the $\sqrt{T^+T^-}$ term found from (16).

Then, using (12), the Γ^2 term can be evaluated from the following equations:

$$\Gamma^4 + 2\xi_2\Gamma^2 + 1 = 0 \tag{17}$$

$$\Gamma^2 = -\xi_2 \mp \sqrt{\xi_2^2 - 1}, \quad \xi_2 = -\frac{(1-T^+T^-)^2 + 2\ AT^+T^-}{2AT^+T^-}. \tag{18}$$

Here, the correct sign for Γ^2 in (18) is also ascertained by enforcing the passivity principle for passive samples; that is, $|\Gamma^2| \leq 1$.

Incorporating the correct T^+T^- and Γ^2 terms evaluated from (16) and (18) into (10) and (11), we derive T^+ and T^- uniquely as

$$T^+ = \frac{1}{\alpha_0}\frac{T^+T^- - \Gamma^2}{m_{11}(1-\Gamma^2)} \tag{19}$$

$$T^- = \frac{1}{\alpha_0}\frac{T^+T^- - \Gamma^2}{u_{22}(1-\Gamma^2)}. \tag{20}$$

B. Determination of Impedance and Propagation Constants

Next, z_w, γ^+, and γ^- can be evaluated from (18) to (20) as

$$z_w = \left(\frac{1+\Gamma^2}{1-\Gamma^2}\right) \mp 2\sqrt{\frac{\Gamma^2}{\left(1-\Gamma^2\right)^2}} \tag{21}$$

$$\gamma^+ = -\frac{\ln(T^+) \mp j\ 2\pi m_{b1}}{L}, \tag{22}$$

$$\gamma^- = -\frac{\ln(T^-) \mp j\ 2\pi m_{b2}}{L} \tag{23}$$

where m_{b1} and m_{b2} are the branch index terms taking natural number values $0, 1, 2, \ldots$ and $\ln(\star)$ indicates the natural logarithm of "$\star$." The branch index values m_{b1} and m_{b2} can be evaluated by using the methodologies in [8] and [17]–[20] briefly discussed in Section I. The correct sign for z_w from (21) can be ascertained by enforcing the passivity principle, that is, $\Re e\{z_w\} \geq 0$, where $\Re e\{\star\}$ denotes the real part of "$\star$."

It is noted that when $T^+ = T^- = T$ for reciprocal samples, the proposed method reduces to the method in [21]. Besides, when $L_{01} = 0 = L_{02}$, our method reduces to the method in [37]. Therefore, our proposed method is general and applicable to determination of both the propagation constant and impedance of reciprocal and non-reciprocal samples.

C. Determination of Transformation Distances L_{01} and L_{02}

Because γ^+, γ^-, and z_w can be evaluated from (21) to (23), evaluating L_{01} and L_{02} is an additional information. After determining T^+ and T^-, the reference plane transformation factors α_{01} and α_{02} can be found from

$$\alpha_{01}^4 = -\frac{1}{\alpha_0^2}\frac{m_{12}}{m_{21}}, \quad \alpha_{02}^4 = -\frac{1}{\alpha_0^2}\frac{u_{21}}{u_{12}}. \tag{24}$$

Because it is seen from (24) that α_{01} and α_{02} terms are functions of the measured S-parameters for a known sample length L (and α_0), it is possible to determine L_{01} and L_{02}

$$L_{01} = \frac{j\ln(\alpha_{01}^4) \mp 2\pi m_{b3}}{4k_0\sqrt{1-(f_c/f)^2}} \tag{25}$$

$$L_{02} = \frac{j\ln(\alpha_{02}^4) \mp 2\pi m_{b4}}{4k_0\sqrt{1-(f_c/f)^2}} \tag{26}$$

where m_{b3} and m_{b4} (just as m_{b1} and m_{b2}) are the branch index terms taking natural number values $0, 1, 2, \ldots$ Since m_{b1} and m_{b2} are multivalued complex variables, the solution for L_{01} and L_{02} will also be multivalued quantities. Since L_{01} and L_{02} are the physical lengths, their values will not change with frequency. Therefore, the correct L_{01} (L_{02}) term can be evaluated from multiple nonharmonic frequencies (at least two nonharmonic frequencies) by recording the same L_{01} (L_{02}) term for each different m_{b3} (m_{b4}) for different frequencies [33]. It is noted that our method essentially does not require evaluation of L_{01} and L_{02} from (25) to (26) to extract γ^+, γ^-, and z_w from (21) to (23). Nonetheless, the determination of L_{01} and L_{02} could be utilized indirectly to evaluate the accuracy of γ^+, γ^-, and z_w measured by our method, as discussed in Section IV-B.

IV. Results and Discussion

A. Measurement Setup

Fig. 2 shows the measurement setup. A Keysight Technologies VNA is used to generate the electromagnetic signals and measure the forward and backward reflection and transmission S-parameters. (The VNA model N9918A can measure S-parameters up to 26.5 GHz with an approximate dynamic range of 90 dB.) Two waveguide sections (X-band, 8.2–12.4 GHz) with lengths greater than $2\lambda_0$, where λ_0 is the free-space wavelength at 8.2 GHz, were connected between the measurement cell and the coax-to-waveguide adapters to suppress the effect of any higher order modes because the theoretical analysis in Section III assumes dominant-mode wave propagation across the cell. Two 3.5-mm phase-stable cables (1 m) were used to propagate electromagnetic signals to and from the coax-to-waveguide adapters. Different X-band waveguide measurement cells, to be discussed in Sections IV-B and IV-C, were used.

The measurement setup was calibrated by the well-known thru-reflect-line (TRL) calibration technique, which is highly applicable for genderless connections such as waveguides [41]. A 9.40-mm waveguide section was operated as the line standard, and a highly reflective short-circuit (unknown reflectivity) was used as the reflect standard. This line standard creates

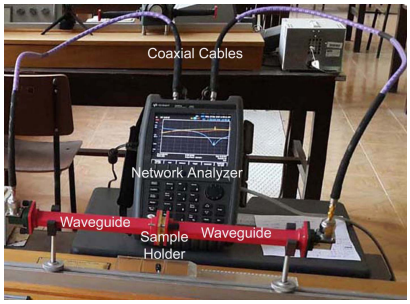

Fig. 2. Photograph of the measurement setup.

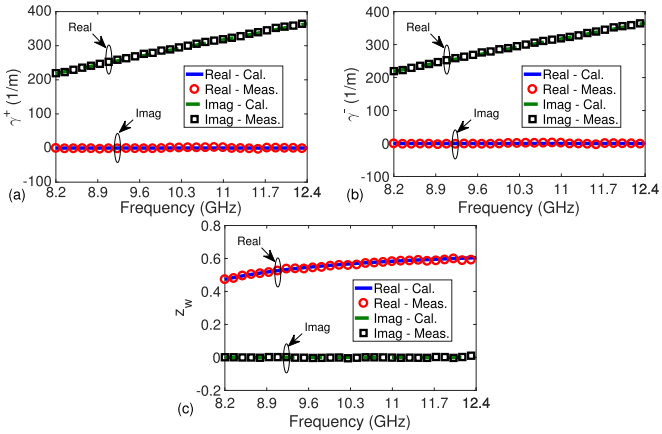

Fig. 3. Frequency dependence of measured (red circle and black square shapes) and calculated (solid blue and dashed green lines) real and imaginary parts of (a) γ^+, (b) γ^-, and (c) z_w of the polypropylene sample with $L = 5.10$ mm.

a maximum phase shift of $\mp 70°$ from 90° (of the thru standard) at the midfrequency of 10.3 GHz. After the calibration, which sets the reference (calibration) planes to the end of the additional waveguide sections, magnitudes of (forward and/or backward) reflection and transmission S-parameters of the thru (or line) standard were measured to be less than -40 dB and greater than -0.03 dB, respectively, over the entire frequency band of interest. These results assure the suitability of the constructed measurement setup for S-parameter measurements in many applications [42].

B. Validation

Before testing the proposed formalism for a non-reciprocal microwave network, it was validated by forward and backward reflection and transmission (calibrated) S-parameter measurements of two low-loss reciprocal dielectric samples (a polypropylene (PP) sample with length $L = 5.10$ mm and a polyvinyl chloride (PVC) sample with length $L = 5.18$ mm) positioned arbitrarily into an empty X-band waveguide straight (the measurement cell) with length $L_g \cong 60.30$ mm. These measurements were repeated five times independently to minimize measurement errors and to perform a standard deviation analysis. Figs. 3 and 4 show, respectively, the frequency dependence of the real and imaginary parts of γ^+, γ^-, and z_w values of the PP and PVC samples extracted by our method using averaged S-parameters. To compare the accuracy of

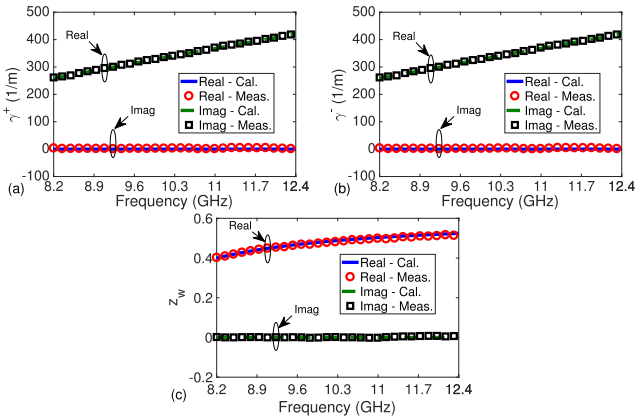

Fig. 4. Frequency dependence of the measured (red circle and black square shapes) and calculated (solid blue and green dashed lines) real and imaginary parts of (a) γ^+, (b) γ^-, and (c) z_w of the polyvinyl chloride sample with $L = 5.18$ mm.

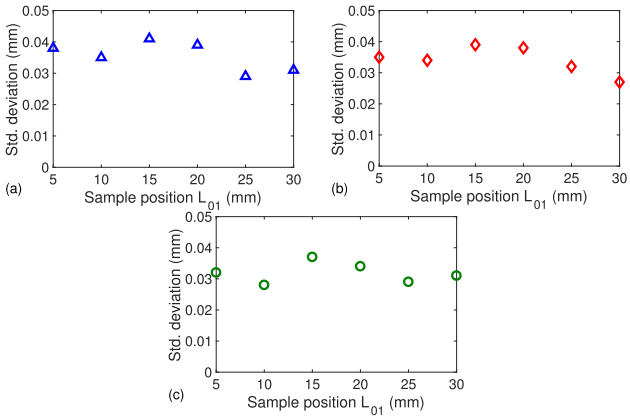

Fig. 5. Standard deviation (Std. deviation) of (a) polypropylene sample with $L = 5.10$ mm, (b) polyvinyl chloride sample with $L = 5.18$ mm, and c) soda–lime glass sample with $L = 2.84$ mm evaluated by the expression in (22).

extracted γ^+, γ^-, and z_w by our method, these values were also calculated using $\varepsilon_r \cong 2.26 - j0.0004$ (9.4 GHz) for the PP sample and $\varepsilon_r = 2.71 - j0.008$ (11.0 GHz) for the PVC sample [43]. The following points are noted from Figs. 3 and 4. First, the real and imaginary parts of the measured γ^+, γ^-, and z_w are in good agreement with the calculated ones. Second, as expected, the measured γ^+ and γ^- using the proposed method are almost identical over entire frequency band, showing the applicability of our method to reciprocal materials.

Because our proposed method can determine the sample position after evaluating L_{01} from (22) [or L_{02} from (23)], in line with the study [33], we also calculated the sample position determined by using L_{01} for the PP and PVC samples using two nonharmonic frequencies. For example, Fig. 5(a) and (b) shows the standard deviation of the position of the PP and PVC samples calculated by our method. Prior information of the position of the sample in the measurement cell was gathered from measurements by a high-precision caliper. It is seen from Fig. 5(a) and (b) that the values of standard deviation of the sample position for the PP and PVC samples are consistent regardless of the sample position, which is in good agreement with the results in Fig. 4(a) and (b) in [33]. We note that the average standard deviation (approximately 0.034 mm) of the sample position for the PVC sample is lower than that (nearly 0.036) for the PP sample. The reason for this is the higher dielectric constant value of the PVC sample, compared to that of the PP sample, for one measurement cell and the same sample positions. This is because the higher the value of the dielectric constant, the greater the value of reflection coefficient, and thus, the better the measurement accuracy (reflection S-parameter will decrease for samples with smaller dielectric constants due to the difficulty of distinguishing such a sample from air). To support this claim, as shown in Fig. 5(c), we also applied our method to evaluate L_{01} of a soda–lime glass sample with $L = 2.84$ mm whose dielectric constant is around 6 [44] (the extracted γ^+, γ^-, and z_w's of this sample are not presented for simplicity). It is noted from Fig. 5(a)–(c) that the average

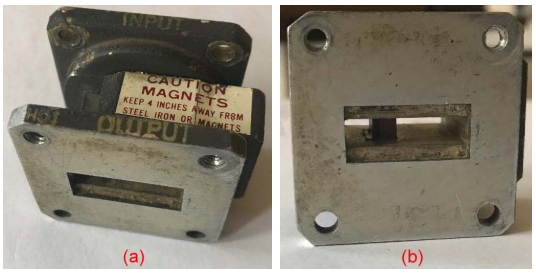

Fig. 6. (a) Perspective-view and (b) front-view photograph of the ferrite-loaded waveguide microwave phase shifter (IEEE© [39], [40]).

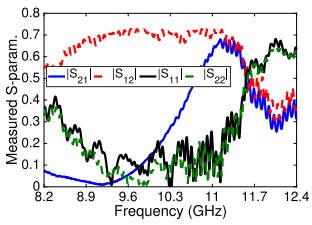

Fig. 7. Magnitudes of measured S-parameters of the ferrite-loaded waveguide phase shifter with $L = 28.7$ mm (Elsevier© [39], [40]).

standard deviation (approximately 0.032 mm) of the sample position for the glass sample is lower than those for the PP and PVC samples, validating the aforementioned claim.

C. Propagation Constant and Impedance Measurements of a Microwave Phase Shifter

After validating our proposed method for γ^+, γ^-, and z_w measurements of sample-loaded (PP and PVC) waveguide sections, we carried out measurements of γ^+, γ^-, and z_w of a non-reciprocal network (an X-band microwave phase shifter with $L = 28.7$ mm). Perspective- and front-view photographs of this shifter are shown in Fig. 6(a) and (b), respectively. Fig. 7 shows the magnitudes of the forward and backward reflection and transmission S-parameters (S_{11}, S_{22}, S_{21}, and S_{12}). It is seen from Fig. 7 that the sample possesses reflection-symmetry property ($|S_{11}| \cong |S_{22}|$) and

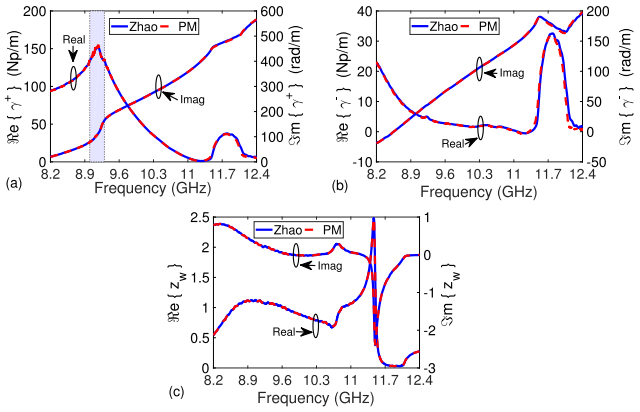

Fig. 8. Frequency dependence of measured real and imaginary parts of (a) γ^+, (b) γ^-, and (c) z_w of the microwave phase shifter by the method [37] (denoted by "Zhao") when $L_{01} = L_{02} = 0$ mm and the proposed method (denoted by "PM").

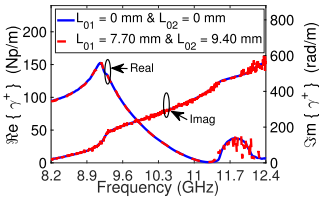

Fig. 9. Frequency dependence of measured real and imaginary parts of γ^+ of the microwave phase shifter with $L = 28.7$ mm by the method in [37] when no additional waveguide straights were present ($L_{01} = L_{02} = 0$ mm) and when the waveguide straights with lengths $L_{01} = 7.70$ mm and $L_{02} = 9.40$ mm were attached to the ends of the microwave shifter.

non-reciprocal property ($|S_{21}| \neq |S_{12}|$). Various combinations of empty X-band waveguide straights with different lengths of 7.70, 9.40, 11.15, and 20.55 mm connected to the ends of the microwave phase shifter were used to construct a measurement cell to test our method.

Then, S-parameter measurements were repeated five times independently to analyze the performance of our proposed method. The frequency variation of standard deviation values is presented in Fig. 10 to demonstrate the performance of our proposed method for different waveguide straight lengths. Fig. 8(a)–(c) shows the extracted γ^+, γ^-, and z_w of this shifter by our proposed method after connecting two waveguide sections with lengths $L_1 = 7.70$ mm and $L_2 = 9.40$ mm to the ends of the phase shifter ($L_g = 45.8$ mm) and by the method (denoted by "Zhao") in the study [37] without additional waveguide sections (e.g., $L_{01} = L_{02} = 0$ mm) using averaged S-parameters. We note the following. First, the extracted γ^+, γ^-, and z_w by our method when $L_1 = 7.70$ mm and $L_2 = 9.40$ mm are in good agreement with those by the method in [37]. Second, the real parts of γ^+, γ^-, and z_w extracted by our method and the method in [37] satisfy the passivity principle ($\Re e\{\gamma^+\} \geq 0$, $\Re e\{\gamma^-\} \geq 0$, and $\Re e\{z_w\} \geq 0$). Third, the real (and imaginary) parts of γ^+ and γ^- are different from each other (consistent with $|S_{21}| \neq |S_{12}|$), thus validating that the microwave phase shifter used in our measurements is a non-reciprocal network.

In order to show the effect of reference-plane transformation distances L_{01} and L_{02} on the extracted γ^+, γ^-, and z_w by the method in [37], this method is applied after two waveguide sections with lengths $L_1 = 7.70$ mm and $L_2 = 9.40$ mm were connected to the ends of the phase shifter. Fig. 9 shows the extracted γ^+ (for brevity, the extracted γ^- and z_w are not shown) obtained by the method in [37]: 1) when no additional waveguide sections were connected ($L_{01} = L_{02} = 0$ mm) and 2) when additional waveguide sections with lengths $L_1 = 7.70$ mm and $L_2 = 9.40$ mm were connected. It is seen from Fig. 9 that the extracted γ^+ by the method in [37] is appreciably affected, especially for higher frequencies (a similar effect was noted in the study in [33]) due to the effect of nonzero L_{01} and L_{02}.

To examine whether different L_{01} and L_{02} combination alters the accuracy of our method, γ^+, γ^-, and z_w were extracted for various combinations of L_{01} and L_{02} compiled from 7.70-, 9.40-, 11.15-, and 20.55-mm waveguide straights. For example, Fig. 10(a) and (b) shows the frequency dependence of the standard deviation values (from average) of the real and imaginary parts of the retrieved γ^+ at some discrete frequencies (for brevity, the extracted γ^- and z_w are not shown) by the proposed method when $L_{01} = 7.70$ mm and $L_2 = 9.40$ mm ($L_g = 45.8$ mm) and when $L_{01} = 11.15$ mm and $L_{02} = 20.55$ mm ($L_g = 60.4$ mm). It is seen from Fig. 10(a) and (b) that the standard deviation in the γ^+ measurements decreases with an increase in L_{01} and L_{02}. It means that, similar to the result given in the study in [33], longer measurement cells should be preferred to improve the measurement accuracy.

Finally, it is noted that the accuracy of our method decreases when the sample (or structure) is low-loss and/or has a smaller L compared with wavelength because it is then challenging to discern m_{b1} and m_{b2} from (22) to (23) [in addition to m_{b3} and m_{b4} from (25) to (26)]. Although this situation requires some prior information about sample loss, many closely separated nonharmonic frequencies could be applied to reduce eliminate this effect and eliminate any error in the estimation of m_{b1} and m_{b2}.

V. Uncertainty Analysis

There are few factors influencing the performance of our proposed method, such as the uncertainty in S-parameters, errors in the sample length and sample position, impact of higher order modes, guide losses and mismatches, air gap between sample lateral surfaces, and the measurement cell. All these uncertainty terms have been intensively studied [9]–[14], [21], [28], [31], [33]. Among these uncertainty terms, our main concern is the analysis of the effects of measured quantities A, C, m_{11}, u_{22}, and L on γ^+, γ^-, and z_w because our method relies on (12)–(23). It is noted that the detection of L_{01} and L_{02} is an additional step in our method. For our goal, the well-known differential uncertainty model, as shown in the following, can be applied, where ^{o} denotes the real or imaginary part; $\chi = \gamma^+$, γ^-, and z_w; p means A, C, m_{11}, and u_{22}; and $\Delta|p|$, $\Delta\theta_p$, and ΔL denote the individual uncertainty terms of $|p|$, θ_p (phase of the p term), and L, respectively.

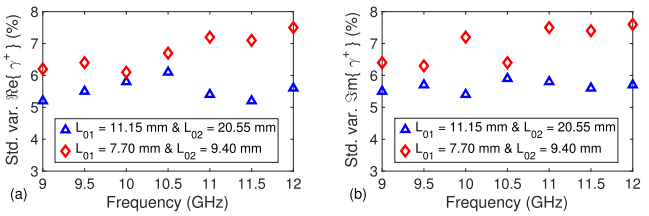

Fig. 10. Frequency dependence of the standard deviation (in percentage) of (a) real and (b) imaginary parts of γ^+ extracted by our method when $L_{01} = 7.70$ mm and $L_{02} = 9.40$ mm and when $L_{01} = 11.15$ mm and $L_{02} = 20.55$ mm.

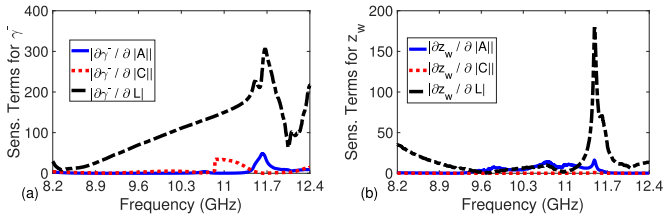

Fig. 11. Frequency dependence of (a) $|\partial\gamma^-/\partial|A||$, $|\partial\gamma^-/\partial|C||$, and $|\partial\gamma^-/\partial L|$ and (b) $|\partial z_w/\partial|A||$, $|\partial z_w/\partial|C||$, and $|\partial z_w/\partial L|$ for the ferrite-loaded microwave phase shifter.

It is seen from the expressions of A in (12), C in (13), m_{11} in (19), and u_{22} in (20) that all these terms are functions of T^+, T^-, and Γ, which all depend on γ^+, γ^-, and z_w, respectively. Assuming that T^+ (T^- and Γ) is complex-differentiable with respect to γ^+ (γ^- and z_w) and following the procedure in the study in [9], $\partial\chi/\partial|p|$, $\partial\chi/\partial\theta_p$, and $\partial\chi/\partial L$ terms can be derived. For example, $\partial\gamma^+/\partial|A|$, $\partial\gamma^-/\partial|A|$, $\partial z_w/\partial|A|$, $\partial\gamma^+/\partial L$, $\partial\gamma^-/\partial L$, and $\partial z_w/\partial L$ can be derived as

$$\frac{\partial\gamma^-}{\partial|A|} = \frac{1}{\dfrac{\partial T^-}{\partial\gamma^-}} \frac{jU_2\dfrac{\partial C}{\partial\Gamma}\theta_A}{U_1U_2 - U_3U_4} \tag{28}$$

$$\frac{\partial\gamma^+}{\partial|A|} = -\frac{U_4\dfrac{\partial T^-}{\partial\gamma^-}}{U_2\dfrac{\partial T^+}{\partial\gamma^+}} \frac{\partial\gamma^-}{\partial|A|} \tag{29}$$

$$\frac{\partial z_w}{\partial|A|} = -\frac{\left(\dfrac{\partial C}{\partial T^+}\dfrac{\partial T^+}{\partial\gamma^+}\dfrac{\partial\gamma^+}{\partial|A|} + \dfrac{\partial C}{\partial T^-}\dfrac{\partial T^-}{\partial\gamma^-}\dfrac{\partial\gamma^-}{\partial|A|}\right)}{\dfrac{\partial C}{\partial\Gamma}\dfrac{\partial\Gamma}{\partial z_w}} \tag{30}$$

$$\frac{\partial\gamma^-}{\partial L} = -\frac{1}{\dfrac{\partial T^-}{\partial\gamma^-}}\left(\frac{2\,k_0\sqrt{1-\left(\frac{f_c}{f}\right)^2}U_2\dfrac{\partial C}{\partial\Gamma}A}{U_1U_2 - U_3U_4} + \frac{\partial T^-}{\partial L}\right) \tag{31}$$

$$\frac{\partial\gamma^+}{\partial L} = -\frac{1}{\dfrac{\partial T^+}{\partial\gamma^+}}\left(\frac{U_4\left(\dfrac{\partial T^-}{\partial L} + \dfrac{\partial T^-}{\partial\gamma^-}\dfrac{\partial\gamma^-}{\partial L}\right)}{U_2} + \frac{\partial T^+}{\partial L}\right) \tag{32}$$

$$\frac{\partial z_w}{\partial L} = -\frac{\left[\dfrac{\partial C}{\partial T^+}\left(\dfrac{\partial T^+}{\partial\gamma^+}\dfrac{\partial\gamma^+}{\partial L} + \dfrac{\partial T^+}{\partial L}\right) + \dfrac{\partial C}{\partial T^-}\left(\dfrac{\partial T^-}{\partial\gamma^-}\dfrac{\partial\gamma^-}{\partial L} + \dfrac{\partial T^-}{\partial L}\right)\right]}{\dfrac{\partial C}{\partial\Gamma}\dfrac{\partial\Gamma}{\partial z_w}} \tag{33}$$

where

$$U_1 = \frac{\partial C}{\partial\Gamma}\frac{\partial A}{\partial T^-} - \frac{\partial A}{\partial\Gamma}\frac{\partial C}{\partial T^-} \tag{34}$$

$$U_2 = \frac{\partial u_{22}}{\partial\Gamma}\frac{\partial m_{11}}{\partial T^+} - \frac{\partial m_{11}}{\partial\Gamma}\frac{\partial u_{22}}{\partial T^+} \tag{35}$$

$$U_3 = \frac{\partial C}{\partial\Gamma}\frac{\partial A}{\partial T^+} - \frac{\partial A}{\partial\Gamma}\frac{\partial C}{\partial T^+} \tag{36}$$

$$U_4 = \frac{\partial u_{22}}{\partial\Gamma}\frac{\partial m_{11}}{\partial T^-} - \frac{\partial m_{11}}{\partial\Gamma}\frac{\partial u_{22}}{\partial T^-}. \tag{37}$$

Other partial differential terms $\partial\chi/\partial|C|$, $\partial\chi/\partial|m_{11}|$, $\partial\chi/\partial|u_{22}|$, $\partial\chi/\partial\theta_p$, and $\partial\chi/\partial L$ are not given here for conciseness. Intermediate partial derivatives in (28)–(37) can be derived using the expressions in (12)–(20).

Before presenting the results for the uncertainty terms $\Delta\gamma^+/\gamma^+$, $\Delta\gamma^-/\gamma^-$, and $\Delta z_w/z_w$, we first performed a sensitivity analysis to evaluate how the γ^+, γ^-, and z_w terms depend on A, C, and L. For example, Fig. 11(a) and (b) shows $|\partial\gamma^-/\partial|A||$, $|\partial\gamma^-/\partial|C||$, $|\partial\gamma^-/\partial L|$, $|\partial z_w/\partial|A||$, $|\partial z_w/\partial|C||$, and $|\partial z_w/\partial L|$. It is seen from Fig. 11(a) and (b) that the extracted terms γ^- and z_w by our method are highly dependent on L (other dependencies also produce similar results; for this reason, they are not shown here for brevity). Stronger dependence of γ^- (and γ^+) and z_w with respect to L will decrease for samples with considerable losses.

Next, we consider the frequency dependence of the real and imaginary parts of all uncertainty terms. Figs. 12 and 13 show the frequency dependence of the real and imaginary parts of $\Delta\gamma^+/\gamma^+$, $\Delta\gamma^-/\gamma^-$, and $\Delta z_w/z_w$ using the extracted parameters of the ferrite-loaded microwave phase shifter (see Fig. 8) for $\Delta L = 0.1$ mm and $\Delta L = 0.2$ mm, assuming that $\Delta|A| = \Delta|C| = \Delta|m_{11}| = \Delta|u_{22}| = 0.02$, $\Delta L = 0.1$ mm, and $\Delta\theta_A = \Delta\theta_C = \Delta\theta_{m11} = \Delta\theta_{u22} = 1^o$ [30], [33]. In Fig. 13(a)–(c), $\Im m\{\star\}$ denotes the imaginary part of "$\star$." The following two important points are noted from the dependencies in Figs. 12 and 13. First, the real and imaginary parts of $\Delta\gamma^+/\gamma^+$, $\Delta\gamma^-/\gamma^-$, and $\Delta z_w/z_w$ considerably change with sample thickness uncertainty ΔL, which is in agreement with the results presented in Fig. 11(a) and (b). Second, the real and imaginary parts of $\Delta\gamma^+/\gamma^+$ and $\Delta\gamma^-/\gamma^-$ in Figs. 12(a) and (b) and 13(a) and (b) inflate around 9 GHz due

$$\frac{\Delta\chi^o}{\chi^o} = \frac{1}{\chi^o}\sqrt{\sum_{p=A,C,m_{11},u_{22}}\left[\left(\frac{\partial\chi^o}{\partial|p|}\Delta|p|\right)^2 + \left(\frac{\partial\chi^o}{\partial\theta_p}\Delta\theta_p\right)^2\right] + \left(\frac{\partial\chi^o}{\partial L}\Delta L\right)^2} \tag{27}$$

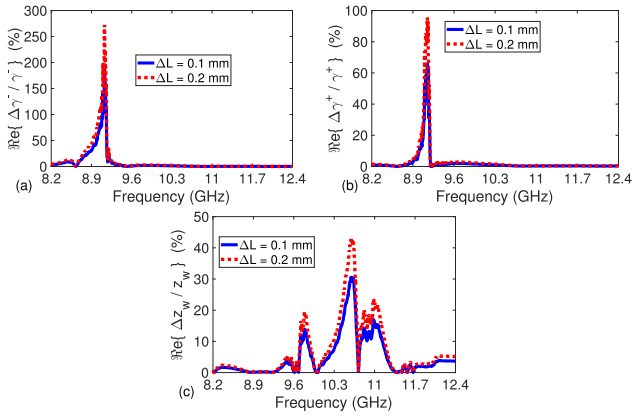

Fig. 12. Percentage changes of (a) $\Re e\{\Delta\gamma^-/\gamma^-\}$, (b) $\Re e\{\Delta\gamma^+/\gamma^+\}$, and (c) $\Re e\{\Delta z_w/z_w\}$ versus frequency for the ferrite-loaded microwave phase shifter for $\Delta L = 0.1$ mm and $\Delta L = 0.2$ mm.

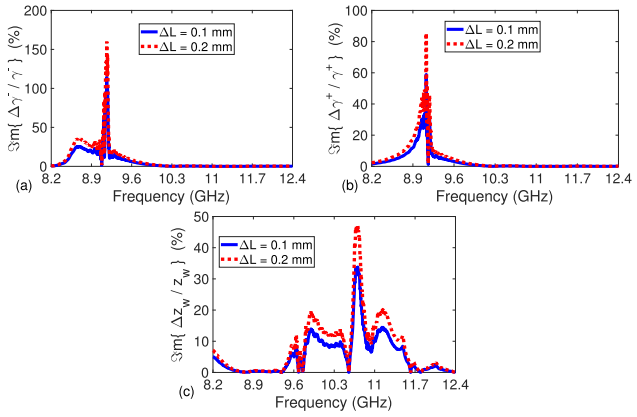

Fig. 13. Percentage changes of (a) $\Im m\{\Delta\gamma^-/\gamma^-\}$, (b) $\Im m\{\Delta\gamma^+/\gamma^+\}$, and (c) $\Im m\{\Delta z_w/z_w\}$ versus frequency for the ferrite-loaded microwave phase shifter for $\Delta L = 0.1$ mm and $\Delta L = 0.2$ mm.

to small variations of $\partial T^-/\partial\gamma^-$ and (especially) $\partial T^+/\partial\gamma^+$, compared with $\partial\Gamma/\partial z_w$ variation [see the denominators of (28)–(33)]. Fig. 14(a) and (b) shows the frequency dependence of $|\partial T^-/\partial\gamma^-|$, $|\partial T^+/\partial\gamma^+|$, and $|\partial\Gamma/\partial z_w|$. It is seen from Fig. 14(a) and (b) that $|\partial T^+/\partial\gamma^+|$ term approaches zero around 9.1 GHz and $|\partial T^-/\partial\gamma^-|$ is considerably smaller than $|\partial\Gamma/\partial z_w|$, both of which we think are the reason for the peaks around 9.1 GHz in Figs. 12(a) and (b) and 13(a) and (b). Finally, small ripples (shown within the shaded region shown light blue color) in Fig. 8(a) in the extracted $\Re e\{\gamma^+\}$ by the proposed method are partly due to very small value of $|\partial T^+/\partial\gamma^+|$ around 9.1 GHz.

It should be noted that uncertainty correlation was not considered in our study. Therefore, this correlation could partly change the overall uncertainty. On the other hand, our method, as other reference-plane-invariant techniques in the studies [21]–[26], [28]–[35] (the method in the study [27] is only applicable for permittivity determination), requires the information of L as seen from the α_0 term in (13) and is limited to γ^+, γ^-, and z_w measurement of reflection-symmetric non-reciprocal samples/networks. It would be very advantageous to determine γ^+, γ^-, and z_w without the information of L_{01} (or L_{02}) and L for reflection-symmetric or reflection-asymmetric non-reciprocal samples/networks. Such a topic is considered as a future study.

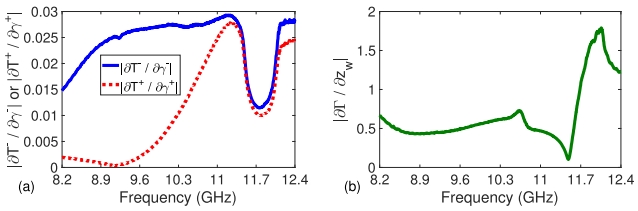

Fig. 14. Frequency dependence of (a) $|\partial T^-/\partial\gamma^-|$ and $|\partial T^+/\partial\gamma^+|$ and (b) $|\partial\Gamma/\partial z_w|$ for the ferrite-loaded microwave phase shifter.

VI. Conclusion

We have proposed transmission–reflection extraction method to determine the forward and backward propagation constants and wave impedance properties of non-reciprocal samples whose exact position L_{01} (or L_{02}) within its cell is not known (position-insensitive). Expressions of these properties derived using the WCM formalism of empty cell and loaded cell with the sample are analytical, meaning that there is no need to apply any numerical technique to evaluate these properties. Next, X-band waveguide measurements of a waveguide straight were first performed to validate our proposed method for reciprocal networks. Then, X-band measurements of a non-reciprocal microwave phase shifter were utilized to extract forward and backward propagation constants and wave impedance of this shifter by our method.

The accuracy of our method was compared with another reference method, which requires exact knowledge of the sample position within its cell. It is noted from this comparison that extracted electromagnetic properties by this reference method were appreciably affected by any incorrect information of L_{01} and L_{02}. Finally, an uncertainty analysis (in addition to sensitivity analysis) was conducted, showing that the accuracy of our method could be increased by precise knowledge of the sample thickness and that its accuracy may decrease when $|\partial T^+/\partial\gamma^+|$ and/or $|\partial T^-/\partial\gamma^-|$ approaches zero. The proposed method can find applications in reference-plane-invariant (i.e., position-insensitive) electromagnetic characterization of microwave phase shifters and chiral metamaterials.

References

[1] S. Trabelsi and S. O. Nelson, "Microwave sensing of quality attributes of agricultural and food products," *IEEE Instrum. Meas. Mag.*, vol. 19, no. 1, pp. 36–41, Feb. 2016.

[2] Z. Meng, Z. Wu, and J. Gray, "Microwave sensor technologies for food evaluation and analysis: Methods, challenges and solutions," *Trans. Inst. Meas. Control*, vol. 40, no. 12, pp. 3433–3448, Aug. 2018.

[3] K. L. Chung and S. Kharkovsky, "Monitoring of microwave properties of early-age concrete and mortar specimens," *IEEE Trans. Instrum. Meas.*, vol. 64, no. 5, pp. 1196–1203, May 2015.

[4] D. Schurig *et al.*, "Metamaterial electromagnetic cloak at microwave frequencies," *Science*, vol. 314, no. 5801, pp. 977–980, Oct. 2006.

[5] F.-Y. Han, T.-J. Huang, L.-Z. Yin, J.-Y. Liu, and P.-K. Liu, "Superfocusing plate of terahertz waves based on a gradient refractive index metasurface," *J. Appl. Phys.*, vol. 124, no. 20, Nov. 2018, Art. no. 204902.

[6] L. F. Chen, C. K. Ong, C. P. Neo, V. V. Varadan, and V. K. Varadan, *Microwave Electronics: Measurement and Materials Characterization*. West Sussex, U.K.: Wiley, 2004.

[7] A. M. Nicolson and G. F. Ross, "Measurement of the intrinsic properties of materials by time-domain techniques," *IEEE Trans. Instrum. Meas.*, vol. IM-19, no. 4, pp. 377–382, Nov. 1970.

[8] W. B. Weir, "Automatic measurement of complex dielectric constant and permeability at microwave frequencies," *Proc. IEEE*, vol. 62, no. 1, pp. 33–36, Jan. 1974.

[9] J. Baker-Jarvis, E. J. Vanzura, and W. A. Kissick, "Improved technique for determining complex permittivity with the transmission/reflection method," *IEEE Trans. Microw. Theory Techn.*, vol. 38, no. 8, pp. 1096–1103, Aug. 1990.

[10] A.-H. Boughriet, C. Legrand, and A. Chapoton, "Noniterative stable transmission/reflection method for low-loss material complex permittivity determination," *IEEE Trans. Microw. Theory Techn.*, vol. 45, no. 1, pp. 52–57, Jan. 1997.

[11] K. J. Bois, L. F. Handjojo, A. D. Benally, K. Mubarak, and R. Zoughi, "Dielectric plug-loaded two-port transmission line measurement technique for dielectric property characterization of granular and liquid materials," *IEEE Trans. Instrum. Meas.*, vol. 48, no. 6, pp. 1141–1148, Dec. 1999.

[12] T. C. Williams, M. A. Stuchly, and P. Saville, "Modified transmission-reflection method for measuring constitutive parameters of thin flexible high-loss materials," *IEEE Trans. Microw. Theory Techn.*, vol. 51, no. 5, pp. 1560–1566, May 2003.

[13] U. C. Hasar and C. R. Westgate, "A broadband and stable method for unique complex permittivity determination of low-loss materials," *IEEE Trans. Microw. Theory Techn.*, vol. 57, no. 2, pp. 471–477, Feb. 2009.

[14] D. A. Houtz, D. Gu, and D. K. Walker, "An improved two-port transmission line permittivity and permeability determination method with shorted sample," in *IEEE Trans. Microw. Theory Techn.*, vol. 64, no. 11, pp. 3820–3827, Nov. 2016.

[15] J. Baker-Jarvis, R. G. Geyer, and P. D. Domich, "A nonlinear least-squares solution with causality constraints applied to transmission line permittivity and permeability determination," *IEEE Trans. Instrum. Meas.*, vol. 41, no. 5, pp. 646–652, Oct. 1992.

[16] S. Kim and J. Baker-Jarvis, "An approximate approach to determining the permittivity and permeability near $\lambda/2$ resonances in transmission/reflection measurements," *Prog. Electromagn. Res. B*, vol. 58, pp. 95–109, 2014.

[17] U. C. Hasar, "Unique retrieval of complex permittivity of low-loss dielectric materials from transmission-only measurements," *IEEE Geosci. Remote Sens. Lett.*, vol. 8, no. 3, pp. 562–564, May 2011.

[18] V. V. Varadan and R. Ro, "Unique retrieval of complex permittivity and permeability of dispersive materials from reflection and transmitted fields by enforcing causality," *IEEE Trans. Microw. Theory Techn.*, vol. 55, no. 10, pp. 2224–2230, Oct. 2007.

[19] J. J. Barroso and U. C. Hasar, "Constitutive parameters of a metamaterial slab retrieved by the phase unwrapping method," *J. Infr. Millim. THz Waves*, vol. 33, no. 2, pp. 237–244, Jan. 2012.

[20] U. C. Hasar, J. J. Barroso, C. Sabah, Y. Kaya, and M. Ertugrul, "Stepwise technique for accurate and unique retrieval of electromagnetic properties of bianisotropic metamaterials," *J. Opt. Soc. Amer. B, Opt. Phys.*, vol. 30, no. 4, pp. 1058–1068, Apr. 2013.

[21] K. Chalapat, K. Sarvala, J. Li, and G. S. Paraoanu, "Wideband reference-plane invariant method for measuring electromagnetic parameters of materials," *IEEE Trans. Microw. Theory Techn.*, vol. 57, no. 9, pp. 2257–2267, Sep. 2009.

[22] U. C. Hasar, "A fast and accurate amplitude-only transmission-reflection method for complex permittivity determination of lossy materials," *IEEE Trans. Microw. Theory Techn.*, vol. 56, no. 9, pp. 2129–2135, Sep. 2008.

[23] U. C. Hasar, "Two novel amplitude-only methods for complex permittivity determination of medium- and low-loss materials," *Meas. Sci. Technol.*, vol. 19, no. 5, Apr. 2008, Art. no. 055706.

[24] U. C. Hasar, C. R. Westgate, and M. Ertugrul, "Noniterative permittivity extraction of lossy liquid materials from reflection asymmetric amplitude-only microwave measurements," *IEEE Microw. Wireless Compon. Lett.*, vol. 19, no. 6, pp. 419–421, Jun. 2009.

[25] U. C. Hasar and Y. Kaya, "Reference-independent microwave method for constitutive parameters determination of liquid materials from measured scattering parameters," *J. Electromagn. Waves Appl.*, vol. 25, nos. 11–12, pp. 1708–1717, Jan. 2011.

[26] U. C. Hasar, J. J. Barroso, Y. Kaya, M. Ertugrul, and M. Bute, "Reference-plane invariant transmission-reflection method for measurement of constitutive parameters of liquid materials," *Sens. Actuators A, Phys.*, vol. 203, pp. 346–354, Dec. 2013.

[27] U. C. Hasar, J. J. Barroso, M. Bute, Y. Kaya, M. E. Kocadagistan, and M. Ertugrul, "Attractive method for thickness-independent permittivity measurements of solid dielectric materials," *Sens. Actuators A, Phys.*, vol. 206, pp. 107–120, Feb. 2014.

[28] U. C. Hasar, Y. Kaya, J. J. Barroso, and M. Ertugrul, "Determination of reference-plane invariant, thickness-independent, and broadband constitutive parameters of thin materials," *IEEE Trans. Microw. Theory Techn.*, vol. 63, no. 7, pp. 2313–2321, Jul. 2015.

[29] Z. Caijun, J. Quanxing, and J. Shenhui, "Calibration-independent and position-insensitive transmission/reflection method for permittivity measurement with one sample in coaxial line," *IEEE Trans. Electromagn. Compat.*, vol. 53, no. 3, pp. 684–689, Aug. 2011.

[30] U. C. Hasar, "Self-Calibrating transmission-reflection technique for constitutive parameters retrieval of materials," *IEEE Trans. Microw. Theory Techn.*, vol. 66, no. 2, pp. 1081–1089, Feb. 2018.

[31] U. C. Hasar, "Determination of complex permittivity of low-loss samples from position-invariant transmission and shorted-reflection measurements," *IEEE Trans. Microw. Theory Techn.*, vol. 66, no. 2, pp. 1090–1098, Feb. 2018.

[32] C. Yang and H. Huang, "Determination of complex permittivity of low-loss materials from reference-plane invariant transmission/reflection measurements," *IEEE Access*, vol. 7, pp. 131865–131872, 2019.

[33] Q. Li, Y. Chen, C. Caisse, A. Horn, and V. G. Harris, "A position-independent approach to accurate measurement of broadband electromagnetic constitutive parameters of magnetodielectric materials," *IEEE Trans. Microw. Theory Techn.*, vol. 68, no. 11, pp. 4940–4950, Nov. 2020.

[34] S. H. Mirjahanmardi, A. M. Albishi, and O. M. Ramahi, "Permittivity reconstruction of nondispersive materials using transmitted power at microwave frequencies," *IEEE Trans. Instrum. Meas.*, vol. 69, no. 10, pp. 8270–8278, Oct. 2020.

[35] T. Mosavirik, M. Soleimani, V. Nayyeri, S. H. Mirjahanmardi, and O. M. Ramahi, "Permittivity characterization of dispersive materials using power measurements," *IEEE Trans. Instrum. Meas.*, vol. 70, pp. 1–8, 2021.

[36] D. M. Pozar, *Microwave Engineering*. West Sussex, U.K.: Wiley, 2011.

[37] R. Zhao, T. Koschny, and C. M. Soukoulis, "Chiral metamaterials: Retrieval of the effective parameters with and without substrate," *Opt. Exp.*, vol. 18, no. 14, Jul. 2010, Art. no. 14553.

[38] U. C. Hasar and M. Bute, "Method for retrieval of electromagnetic properties of inhomogeneous reciprocal chiral metamaterials," *IEEE Trans. Antennas Propag.*, vol. 68, no. 7, pp. 5714–5717, Jul. 2020.

[39] U. C. Hasar, Y. Kaya, G. Ozturk, and M. Ertugrul, "Propagation constant measurements of reflection-asymmetric and nonreciprocal microwave networks from S-parameters without using a reflective standard," *Measurement*, vol. 165, Dec. 2020, Art. no. 108126.

[40] U. C. Hasar, Y. Kaya, and M. Ertugrul, "Measurement of propagation characteristics of nonreciprocal networks/lines using a line–line method," *IEEE Trans. Electromagn. Compat.*, vol. 63, no. 4, pp. 1240–1247, Aug. 2021.

[41] G. F. Engen and C. A. Hoer, "Thru-reflect-line: An improved technique for calibrating the dual 6-port automatic network analyzer," *IEEE Trans. Microw. Theory Techn.*, vol. MTT-27, no. 12, pp. 983–987, Dec. 1979.

[42] D. K. Ghodgaonkar, V. V. Varadan, and V. K. Varadan, "Free-space measurement of complex permittivity and complex permeability of magnetic materials at microwave frequencies," *IEEE Trans. Instrum. Meas.*, vol. 39, no. 2, pp. 387–394, Apr. 1990.

[43] B. Riddle, J. Baker-Jarvis, and J. Krupka, "Complex permittivity measurements of common plastics over variable temperatures," *IEEE Trans. Microw. Theory Techn.*, vol. 51, no. 3, pp. 727–733, Mar. 2003.

[44] U. C. Hasar and M. Bute, "Electromagnetic characterization of thin dielectric materials from amplitude-only measurements," *IEEE Sensors J.*, vol. 17, no. 16, pp. 5093–5103, Aug. 2017.